Scaled Polynomial Expression for Self-Diffusion Coefficients for Water, Benzene, and Cyclohexane over a Wide Range of Temperatures and Densities

Ken Yoshida,*,† Nobuyuki Matubayasi,‡,§ Yasuhiro Uosaki,† and Masaru Nakahara‡

Department of Chemical Science and Technology, Faculty of Engineering, University of Tokushima, 2-1 Minamijosanjima-cho, Tokushima 770-8506, Japan, Institute for Chemical Research, Kyoto University, Uji, Kyoto, 611-0011, Japan, and Japan Science and Technology Agency (JST), CREST, Kawaguchi, Saitama 332-0012, Japan

Self-diffusion coefficients D for water, benzene, and cyclohexane were determined in high-temperature conditions along the liquid branch of the coexistence curve and in supercritical conditions including an extremely low density region. The diffusion data available in literature were compared and evaluated. A fifth-order polynomial for ln D with the single variable T^{-1} ($\ln(D/10^{-9}\ m^2 \cdot s^{-1}) = a_0 + a_1x + a_2x^2 + a_3x^3 + a_4x^4 + a_5x^5$ with $x = 1000/(T/K)$) was found to provide good fitting along the liquid branch of the coexistence curve. A single polynomial function for the scaled quantity $\rho D/T^{1/2}$ with the two variables, density ρ and temperature T^{-1} (third-order polynomial of ρ and T^{-1} and the cross terms), can universally represent the diffusion data over a wider range including both the gas−liquid coexistence and the extremely low density conditions. The function gives a reliable and reasonable behavior of D in the medium-density supercritical states in which the experimental uncertainty is rather large due to the severe conditions. The temperature and density differentials thus obtained were used to shed light on the effect of hydrogen bonding that makes water different from nonpolar organic liquids. The temperature dependence of the self-diffusion coefficient for water is larger than those for organic liquids, due to the large contribution of the attractive hydrogen-bonding interaction. The density dependence is larger for organic liquids than that for water.

1. Introduction

The self-diffusion coefficient D is defined for the mass-transport process and is one of the most fundamental dynamic processes in relation to reaction dynamics in fluids. The self-diffusion in fluids arises from a series of dynamic intermolecular interactions in cages or shells, and thus the self-diffusion data in fluids are of decisive importance to get insight into the microscopic interactions in fluids from the dynamic viewpoint.[1−4] The self-diffusion data have been compiled as a function of the temperature to elucidate the competition of the kinetic energy against the interaction potential energy. The self-diffusion data have been accumulated also as a function of the density to investigate the effect of the frequency of interactions and collisions that are controlled by the number of neighboring molecules and reflected upon the time correlation function of the velocity. Thus, to characterize the states of the interactions that depend on temperature and density in sub- and supercritical conditions, it is of great importance to examine the contributions of the temperature and density effects on the self-diffusion coefficients. The static structure in supercritical water is beyond the van der Waals picture because of the presence of the hydrogen bonding[5,6] and essentially differs from those in common molecular liquids like benzene.[7] However, it is unclear as of yet how the hydrogen-bonding effects of different interactions are manifested in the temperature and density dependencies of dynamic properties. Reliable and good-behavior fitting functions enable us to discuss the temperature and density derivatives that reflect the dynamic intermolecular interactions. The compiled data for water[8−19] and nonpolar organic liquids, benzene[19−25] and cyclohexane,[16,19,23,25−27] are analyzed to formulate the most reliable fitting function.

A number of functions have been proposed to fit the self-diffusion coefficient data. They have been applied and tested for a variety of gases and liquids.[8−38] The fitting functions can be categorized into the following types; (i) the Arrhenius type,[8−12,15,16,20,24,26] (ii) the scaling to the hard-sphere model,[12,13,22,27−29,35−38] (iii) the simple hydrodynamic model or modified ones,[8,11−14,17,19,24,26,27,35,38] (iv) the molar-volume type,[11,12] (v) explicit terms of density and temperature,[13,21,23] (vi) the density expansion type,[14,30−35] and (vii) the gas kinetic theory with collision integrals.[14,18,24,25,31,32,36−38] The choice of the fitting function is based on the region of the thermodynamic states in which the function can appropriately represent the temperature and density dependencies of the self-diffusion coefficients. Some of them are based on physical concepts or meaning, but some others are simply phenomenological models. Typically, i−v have been used in the high-density, liquid-like conditions, and vi and vii in the low-density gas-like conditions. Here we develop approach ii to a large extent. In recent studies, the self-diffusion coefficients were measured for water and two common molecular liquids, benzene and cyclohexane, in sub- and supercritical states through the two-fold variation of absolute temperature and the hundred-fold variation of density.[17−19,25] While the thermodynamic states in which the self-diffusion coefficient exists were largely extended, fitting functions to represent the self-diffusion coefficients over such a wide range of thermodynamic states has not yet been proposed. In this study, we attempt to find some function that can universally fit the

* Corresponding author. E-mail address: yoshida@chem.tokushima-u.ac.jp. Tel.: +81-88-656-7669. Fax: +81-88-655-7025.
† University of Tokushima.
‡ Kyoto University.
§ Japan Science and Technology Agency.

10.1021/je100206s © 2010 American Chemical Society
Published on Web 05/10/2010

Table 1. Experimental Literature on the Self-Diffusion Coefficients for Fluids along the Liquid Branch of the Coexistence Curve

fluid	*t*/°C	method	authors	year	ref
light water	27 to 360	NMR	Hausser, Maier, and Noack	1966	8[a]
	−31 to 25	NMR	Gillen, Douglass, and Hoch	1973	9[b]
	1 to 45	tracer	Mills	1973	10
	10 to 225	NMR	Krynicki, Green, and Sawyer	1979	12[c]
	25 to 90	tracer	Easteal, Price, and Woolf	1989	15
	15 to 56	NMR	Holz, Heil, and Sacco	2000	16
	30 to 350	NMR	Yoshida, Matubayasi, and Nakahara	2008	19
heavy water	5 to 45	tracer	Mills	1973	10
	10 to 200	NMR	Wilbur, DeFries, and Jonas	1976	11
	30 to 350	NMR	Yoshida, Matubayasi, and Nakahara	2008	19
benzene	15 to 55	tracer	McCool, Collings, and Woolf	1972	20
	55 to 60	tracer	Collings and Woolf	1975	21[d]
	30 to 160	NMR	Parkhurst and Jonas	1975	22[e]
	30 to 100	NMR	Polsin and Weiss	1990	23
	30 to 250	NMR	Yoshida, Matubayasi, and Nakahara	2008	19
cyclohexane	15 to 55	tracer	McCool and Woolf	1972	26
	40 to 110	NMR	Jonas, Hasha, and Huang	1980	27[f]
	22 to 120	NMR	Polsin and Weiss	1990	23
	15 to 55	NMR	Holz, Heil, and Sacco	2000	16
	30 to 250	NMR	Yoshida, Matubayasi, and Nakahara	2008	19

[a] Data at (70 to 190) °C are omitted to obtain the best-fit parameters for eq 1. [b] The data at (0 to 25) °C are used for the recommended values in ref 15. [c] Data at (80 to 220) °C are omitted to obtain the best-fit parameters for eq 1. [d] Revision on ref 20. [e] Data at (70 to 160) °C are omitted to obtain the best-fit parameters for eq 1. [f] Data at (60 and 110) °C are omitted to obtain the best-fit parameters for eq 1.

Table 2. High-Temperature NMR Studies on the Self-Diffusion Coefficients for Fluids in the Supercritical Conditions Including the Extremely Low Density Region

	t	*ρ*			
fluid	°C	g·cm^{-3}	authors	year	ref
light water	400 to 700	0.10 to 0.70	Lamb, Hoffman, and Jonas	1981	14
	400	0.071 to 0.25	Yoshida, Wakai, Matubayasi, and Nakahara	2005	17
	200 to 400	0.004 to 0.056	Yoshida, Matubayasi, and Nakahara	2006	18
heavy water	400	0.10 to 0.25	Yoshida, Wakai, Matubayasi, and Nakahara	2005	17
benzene	280 to 410	0.10 to 0.30	Asahi and Nakamura	1997	24
	150 to 400	0.007 to 0.21	Yoshida, Matubayasi, and Nakahara	2009	25
cyclohexane	150 to 400	0.005 to 0.15	Yoshida, Matubayasi, and Nakahara	2009	25

diffusion coefficient over a wide range from ambient to the supercritical states including the extremely low density region.

The thermodynamic region of great interest is the sub- and supercritical conditions in the medium- to high-density range in which the dynamic interactions cannot be categorized simply as "gas-like" or "liquid-like." To reduce carbon dioxide emission by technological innovation, the formulation in the thermodynamic region is essential for a high-efficiency plant and process designs. Scientifically, our recent computational study has elucidated that the self-diffusion shows a turnover from the "in-shell" type to the "mobile-shell" type.[39] The in-shell type represents the velocity relaxation within the solvation shell at high enough densities, and the mobile-shell type represents the velocity relaxation slower than that of the solvation shell structure at low densities. In the supercritical medium-density region where the turnover is observed, the solvation shell does exist because the density is not so low as that for the binary interaction, and the solvation shell is not strong enough to confine the diffusing molecule for a long time due to the high temperature. Though the medium- to high-density region is of great interest from a viewpoint of the self-diffusion and the solvation shell structure as mentioned above, it is extremely difficult to carry out reliable experiments in this region. For water the supercritical conditions above the critical density were covered by the pioneering work by Lamb et al.[14] To consistently connect the self-diffusion data from the low- to high densities, we process the data in the following two steps. First we establish a function along the liquid branch of the coexistence curve, and the data in supercritical states are fitted to a universal function together with those along the coexistence curve established in the first step. A function specific to the coexistence curve is the most needed for engineering and scientific purposes as seen in the previous intensive studies.[8−17,19−24,26,27] For example, it is related to hydrothermal reactions where the density can be continuously and uniquely controlled by the temperature regulation.[40−44] In the second step, the reliable data established in the first step on the coexistence curve at high temperatures play an important role in keeping consistency from the low-temperature and high-density region to the high-temperature and low-density region necessary for continuous and quantitative analysis in engineering, chemistry, and physics as is demonstrated in this paper.

In the following section, the data sources are summarized, the procedure for the data processing is described, and the literature data are compared. In Sections 3.1 and 3.2, the data at high temperatures are discussed based on the fitting curves obtained along the coexistence curve and the whole range of the thermodynamic states, respectively. Conclusions are given in Section 4.

2. Data Analysis

2.1. Data Sources. The references reporting the self-diffusion data along the liquid branch of the coexistence curve are summarized in Table 1. In addition to the high-temperature data, the widely recognized reference data near the ambient conditions are included in Table 1. The references on the supercritical states are listed in Table 2. The data in the density region higher than the liquid branch of the coexistence curve are included in the fitting of the data in the supercritical states

Table 3. Self-Diffusion Coefficients at Densities above the Coexistence Curve Used to Determine the Parameters in Equation 2

	t	ρ			
fluid	°C	g·cm^{-3}	authors	year	ref
water	4 to 60	1.00 to 1.11	Harris and Woolf	1980	13
	10 to 200	1.00 to 1.22[a]	Wilbur, DeFries, and Jonas	1976	11[a]
benzene	15 to 55	0.86 to 0.92	McCool, Collings, and Woolf	1972	20
	55 to 60	0.84 to 0.94	Collings and Woolf	1975	21[b]
cyclohexane	15 to 55	0.75 to 0.81	McCool and Woolf	1972	26
	40 to 110	0.69 to 0.83	Jonas, Hasha, and Huang	1980	27
	22 to 120	0.73 to 0.85	Polsin and Weiss	1990	23

[a] The data measured for heavy water. Their data are normalized by the ratio by the $D_{ave,fit}$ value for eq 1 for light water and the D value for heavy water along the coexistence curve at each temperature. The density of heavy water is normalized to that for light water by the ratio of the densities on the coexistence curve. [b] Revision on ref 20.

Table 4. Recommended Fitting Parameters for Equation 1[a]

	a_0	a_1	a_2	a_3	a_4	a_5
light water	15.0723	−15.5922	8.81532	−2.70394	0.41007	−0.0258761
heavy water	30.4508	−46.6146	33.5991	−12.5420	2.34227	−0.1758570
benzene	23.8834	−24.7707	10.4742	−1.65375	−0.0540921	0.0268665
cyclohexane	54.4316	−85.3141	58.2964	−20.4605	3.60858	−0.255367

[a] The parameters give the D values in 10^{-9} m^2·s^{-1}.

in Section 2.2.2. The references in the high-density region used in this step are listed in Table 3.

2.2. Data Processing. 2.2.1. Liquid Branch of Coexistence Curve. Now we describe the procedures to obtain the best-fit curve of the Arrhenius type by averaging the literature values on the liquid branch of the coexistence curve. The D values in each literature are fitted to an Arrhenius-type function to smooth the experimental uncertainties. The fitted curve for each literature is normalized to the D value at the calibration temperature so that the differences in the calibration data used by various groups are canceled. Then the average among literatures is taken, and the averaged values are fitted to the Arrhenius-type function to obtain the best-fit curve. Finally the curve is normalized so that it gives the most recommended value for each substance at room temperature.

The details of the data processing are as follows. First, the self-diffusion data in each literature (D_{exp}) are fitted to the Arrhenius-type function of a polynomial of the inverse of the temperature with the number of the fitting parameter of n expressed as

$$\ln(D_{fit}/10^{-9}\ \mathrm{m^2\cdot s^{-1}}) = \sum_{i=1}^{n} a_{i-1}(1000/(T/\mathrm{K}))^{i-1} \quad (1)$$

where the D_{fit} value, expressed in 10^{-9} m^2·s^{-1}, is the experimental ($D_{exp,fit}$) or the average ($D_{ave,fit}$) value of D for the fitting. The number n of the fitting parameters is chosen depending on the temperature range covered in each literature. For light water $n = 4$ for refs 10, 15, and 16 and $n = 6$ for refs 8, 12, and 19. For heavy water $n = 3$ for ref 10, $n = 4$ for ref 11, and $n = 6$ for ref 19. For benzene $n = 4$ for ref 20 with refs 21, 22, and 23 and $n = 6$ for ref 19. For cyclohexane $n = 4$ for refs 16, 26, 27, and 23 and $n = 6$ for ref 19. The interpolated fitted self-diffusion values ($D_{exp,fit}$) with 5 °C steps up to 50 °C and with 10 °C steps above 50 °C are used for the averaging below. To use the same calibration point for all of the literature values, the fitting curve for each literature is normalized so that the $D_{exp,fit}$ value at the calibration temperature is the same for all of them. The calibration temperature is 30 °C for light water, heavy water, and benzene and 40 °C for cyclohexane. The calibration temperature of (30 or 40) °C is adopted since some of the references do not cover 25 °C (Table 1). The D value at the calibration temperature is arbitrary, because the fitting curve for the average of literature values is normalized to the accepted values at 25 °C at the final step as described below. In early high-temperature NMR studies, the data in some thermodynamic states are different from those in other literature and would reduce the consistency between the data in the temperature range and those in the higher temperature range. The data deviating from the high-precision values recently reported[19] by more than 5 % are excluded from averaging. The discarded data regions are shown in the notes for Table 1. The final averaged D values (D_{ave}) are obtained from the average of the $D_{exp,fit}$ values among literature values. Then D_{ave}, obtained at intervals of 5 °C up to 50 °C, and at intervals of 10 °C above 50 °C, are fitted to the fifth-order Arrhenius-type function; this is the fitted value, $D_{ave,fit}$. The fitting curve for each literature is normalized so that the $D_{ave,fit}$ value at 25 °C gives the same value as the most reliable self-diffusion data; $D = 2.299\cdot10^{-9}$ m^2·s^{-1} for light water,[10] $1.872\cdot10^{-9}$ m^2·s^{-1} for heavy water,[10] $2.207\cdot10^{-9}$ m^2·s^{-1} for benzene,[20] and $1.450\cdot10^{-9}$ m^2·s^{-1} for cyclohexane.[26] The fitting parameters for eq 1 thus obtained are listed for each liquid in Table 4. The rms (root-mean-square) of relative deviations for light water, heavy water, benzene, and cyclohexane is 0.8 %, 0.4 %, 0.4 %, and 0.3 %, respectively, where the rms is estimated as $[(1/n)\sum^n(100(D_{ave} - D_{ave,fit})/D_{ave,fit})^2]^{1/2}$, and the number of the data points (n) is 41, 40, 28, and 28 for light water, heavy water, benzene, and cyclohexane, respectively.

2.2.2. Supercritical Conditions Including Extremely Low Density Regions. The data in the supercritical states are fitted to a function with the two variables, the density ρ and the temperature inverse T^{-1}. To make consistent the data in the subcritical and the supercritical regions and to reliably separate the density and temperature contributions, the self-diffusion data along the coexistence curve established above and those at high-densities listed in Table 3 are all included in the data-fitting process. This leads us to discuss separately the density and temperature contributions as shown below. In supercritical conditions, no data are screened out before fitting, because the experimental uncertainties in the supercritical conditions are larger than those in the subcritical conditions.

The function is based on the scaling to the hard-sphere model[1,2,4,45] as,

$$\rho D/\sqrt{T} = \sum_{i=1}^{4}\sum_{j=1}^{4} a_{ij}\rho^{i-1}x^{j-1} \quad (2)$$

where $x = 1000/(T/\mathrm{K})$. Here the units of D and ρ are in 10^{-9} $m^2 \cdot s^{-1}$ and $g \cdot cm^{-3}$, respectively. The terms consist of the third-order polynomials of ρ and T^{-1}, and the cross terms of these variables. In eq 2, the quantity on the left-hand side, $\rho D/T^{1/2}$, is an invariant quantity against temperature change in the hard-sphere model. The terms dependent on ρ and T^{-1} are incorporated to take account of the intermolecular interactions as well as the higher-order multibody collisions rather than the binary ones. The parameters in eq 2 determined for T in K, D in 10^{-9} $m^2 \cdot s^{-1}$, and ρ in $g \cdot cm^{-3}$ are listed in Table 5. Whereas the parameters in Tables 4 and 5 reflect some physical meanings in principle, it is not straightforward to clarify the meanings through the comparison between parameters because a number of parameters are required to fit a wide range of T and ρ. Instead, we scrutinize the physical meanings on the basis of the overall behavior of the forms of the functions in terms of the apparent activation energy obtained from eq 1 and the T and ρ derivatives obtained from eq 2.

2.3. Data Evaluation. Now we summarize the data evaluation based on the results of the data processing in Section 2.2. The literature data are evaluated by the deviation of the literature values ($D_{\mathrm{exp,fit}}$) from the best-fit value ($D_{\mathrm{ave,fit}}$) obtained as described above. The deviations are illustrated in Supporting Information (SI, Figure S1). The $D_{\mathrm{exp,fit}}$ values used for the evaluation here are the values fitted to the Arrhenius-type function using literature data. These are normalized so that the average among literature data becomes equal to the best-fit value. For light water in the high temperature range of (200 to 350) °C, the data by Hausser et al.[8] and those by Yoshida et al.[19] are in good agreement. In the medium temperature range of (100 to 200) °C, the data by Hausser et al.[8] and those by Krynicki et al.[12] overestimate the D values, and they are omitted from the present data processing (open symbols in Figure S1a of the SI). Probably, the difference arises from the convection effect in the earlier studies.[8,12] In the recent study[19] the convection effect was minimized by using the vertically symmetric heating system; the convection effect becomes smaller at higher temperatures as a result of larger self-diffusion coefficients.[8] Nevertheless, the discrepancies are less than or comparable to the experimental uncertainties stated in the earlier works; the uncertainties amount to 10 %. The agreement among the literature values below the boiling point is better than that at higher temperatures.

Table 5. Fitting Parameters for Equation 2[a]

	water	benzene	cyclohexane
a_{11}	3.17395	1.008971	−0.6765
a_{21}	0.338985	11.32978	−36.4906
a_{31}	−6.06114	−8.13065	102.8376
a_{41}	3.389694	−9.18857	−68.2323
a_{12}	−3.06059	0.522215	2.579769
a_{22}	−4.4143	−21.2237	64.45348
a_{32}	22.12712	27.11988	−178.027
a_{42}	−13.867	−1.25601	115.5202
a_{13}	1.823286	−0.53989	−1.4283
a_{23}	3.144772	11.64412	−36.3383
a_{33}	−14.654	−18.1626	98.90356
a_{43}	9.105139	5.332843	−63.8094
a_{14}	−0.41778	0.112001	0.245717
a_{24}	−0.4676	−1.91765	6.455743
a_{34}	2.573378	3.235493	−17.4949
a_{44}	−1.6036	−1.24222	11.28953

[a] The parameters give the D values in 10^{-9} $m^2 \cdot s^{-1}$ with ρ in $g \cdot cm^{-3}$ and T in K.

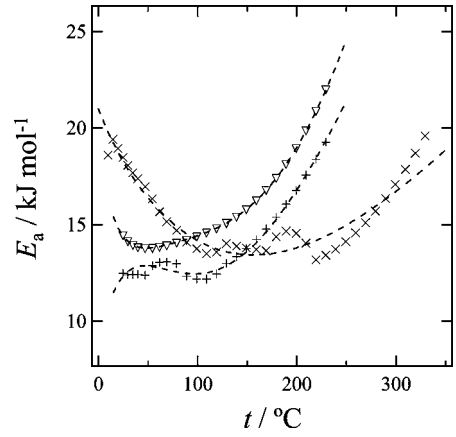

Figure 1. Activation energy E_a of the self-diffusion coefficients along the coexistence curve. The dashed curves are obtained from D fitted to eq 1. The symbols are those obtained as a reference by the linear fitting of the five D values at the neighboring temperatures: ×, water; +, benzene; ▽, cyclohexane.

For the case of heavy water (^2H_2O) reported in ref 11, the deviation shown in Figure S1c of the SI is within the uncertainty (± 5 % to ± 10 %). The deviations for benzene and cyclohexane are plotted in Figure S1, parts d and e, of the SI, respectively. The D values for benzene are in good agreement with each other, except for the data by Parkhurst et al.[22] at higher temperatures. Note that the data by Parkhurst et al. are for deuterated benzene and that they are normalized to the normal benzene data at 30 °C to correct the H/D isotope effect of 5 % at room temperature.[46] Since there are no high-temperature studies on D for both normal and deuterated benzene with high-enough precision to discuss the isotope effect, here we assumed that the temperature dependence of the isotope effect is negligible over the temperature range covered in ref 22 ((30 to 160) °C). This assumption is based on the previous studies showing that the temperature dependence of dynamic isotope effect determined near room temperature is small for benzene and other nonpolar and polar substances.[46] A large decrease in the isotope effect was observed only when the dynamics is strongly controlled by the intermolecular interaction, as in the case of water[17,47] and nonpolar substances at very low temperatures.[48,49] In the case of cyclohexane, the literature values are in good agreement.

3. Results and Discussion

3.1. Liquid Branch of Coexistence Curve. As described in Section 2, the Arrhenius-type function, eq 1, with six parameters (fifth-order polynomial) can successfully fit the average of the experimental values as shown in the SI (Figure S2). By taking advantage of the parameters for the Arrhenius-type function determined as described in Section 2, the temperature dependence of the self-diffusion coefficient can be discussed in terms of the apparent activation energy. The apparent activation energy for the self-diffusion along the coexistence curve, taken as a measure for the temperature effect, can be obtained by differentiating D with respect to T^{-1} as

$$E_a = -R\left(\frac{\partial \ln D}{\partial(1/T)}\right)_{\mathrm{coex}} \quad (3)$$

In Figure 1, we show the apparent activation energy E_a obtained by adopting eq 1 for D for light water. The dashed curve is the one obtained by eq 1, and the crossed symbols are the ones obtained as a reference by the linear fitting of the five D values at the neighboring temperatures. The E_a value for water decreases with increasing temperature in the low-temperature

region near the ambient condition and *increases* at high temperatures toward the critical point. The large E_a value near the ambient temperature is due to the presence of the strong hydrogen-bonding network that serves as a barrier for the diffusing water molecules. The E_a value decreases with increasing temperature as a consequence of the breakage of the hydrogen bonding. The E_a value *increases* at high temperatures above 250 °C and below the critical one because the density expansion per temperature becomes large in this region. It is to be noted that, whereas the apparent activation energy for the self-diffusion is discussed in relation to the jump of a diffusing species out of a cage into a void, it is unreasonable to assume that (10 to 30) % of the total number of molecules are in the middle of such an activated state, in correspondence to the activation energy of 10 kJ·mol^{-1}.[3] A more natural molecular picture is that the displacement of a molecule in fluids is caused by the forces and torques due to attraction and repulsion with the neighboring molecules to which the diffusing molecule is continuously subject. A molecule is displaced by changing the

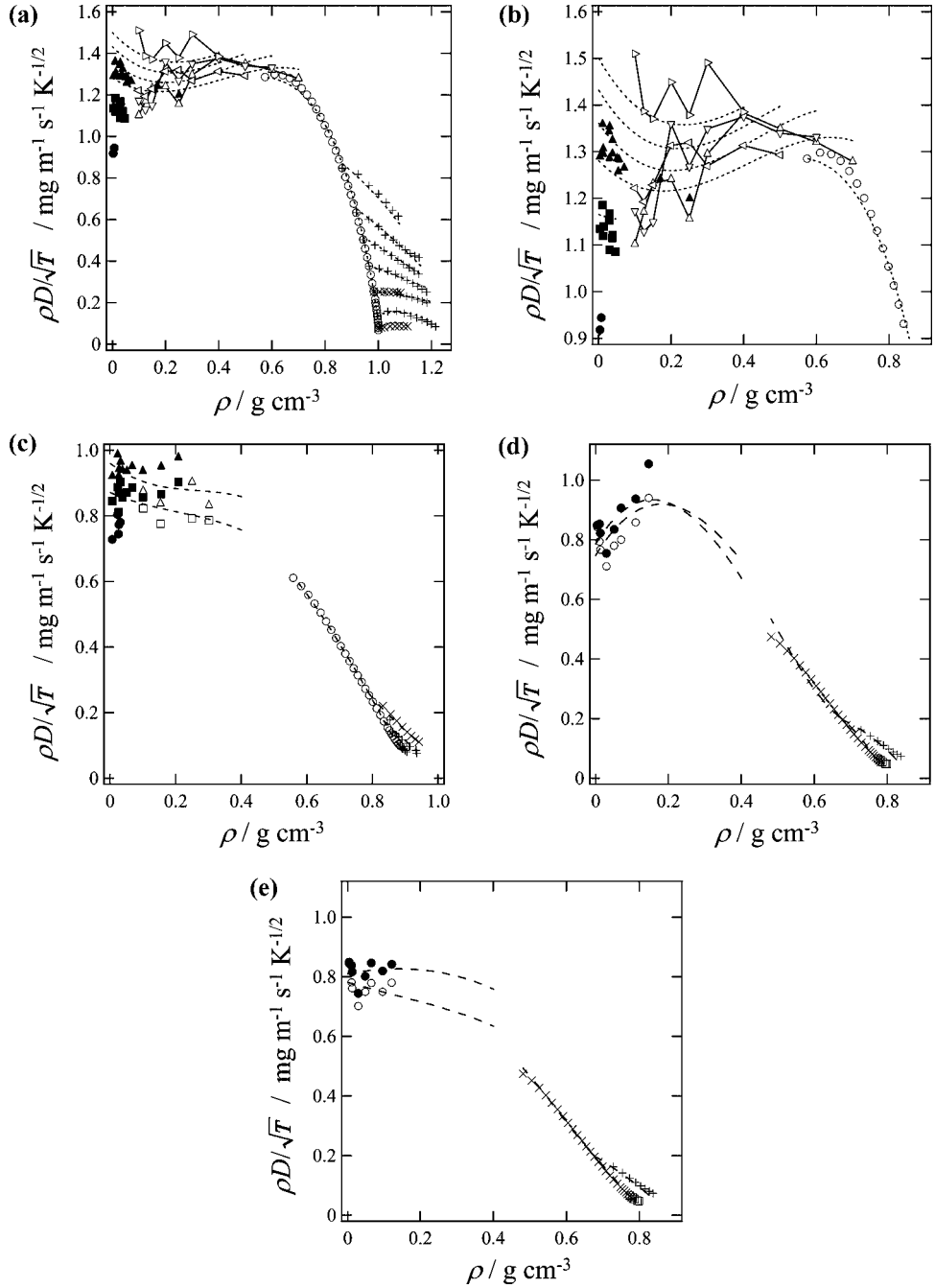

Figure 2. Product $\rho D/T^{1/2}$ for in sub- and supercritical fluids. (a) Water: +, ref 11; ×, ref 13; ○, the best-fit values for eq 1 along the liquid branch of the coexistence curve; ●, ref 18 at 200 °C; ■, ref 18 at 300 °C; ▼, refs 17 and 18 at 400 °C; △, ref 14 at 400 °C; ▽, ref 14 at 500 °C; open left-pointing triangle, ref 14 at 600 °C; open right-pointing triangle, ref 14 at 700 °C. The dashed curves in the medium- to low-density region are the fitting results of eq 2 and are for (700, 600, 500, and 400) °C from top to the bottom. (b) Enlarged view of a in supercritical states. (c) Benzene: +, ref 20 at 15 °C; ×, ref 23 at 100 °C; ○, the best-fit values for eq 1 along the liquid branch of the coexistence curve; ●, ref 25 at 200 °C; ■, ref 25 at 300 °C; ▼, ref 25 at 400 °C; □, ref 24 at 300 °C; △, ref 24 at 400 °C. (d) Cyclohexane with no density adjustment: □, ref 26 at 25 °C; +, ref 23 at 120 °C; ×, the best-fit values for eq 1 along the liquid branch of the coexistence curve; ○, ref 25 at 300 °C; ●, ref 25 at 400 °C. (e) Cyclohexane with density adjustment: the symbols are the same as in d. For the density correction for cyclohexane, see the text. The dashed curves in c−e in the medium- to low-density region are the fitting results of eq 2 and are for (400 and 300) °C from top to the bottom (for d, from top to the bottom at the density lower than the intersection).

direction abruptly and alternately, rather than by instantaneous and discrete jumps.

A comment is made here on the oscillatory nature of the polynomials. When a polynomial is adopted as a fitting function, some nonsmooth behaviors resulting from the oscillatory nature of the polynomials are unavoidable. In the present results, the oscillatory behavior is successfully minimized for water and cyclohexane (0.1 kJ·mol^{-1}) by taking advantage of the multistep smoothing of the fitting function, whereas a slight oscillatory behavior remains for benzene (1 kJ·mol^{-1}). In view of the experimental uncertainties and their amplifications by the differentiation with respect to temperature, the oscillatory behaviors of 1 kJ·mol^{-1} are not essential and can be ignored for a variety of applications.

3.2. Supercritical Conditions Including Extremely Low Density Regions. 3.2.1. Quality of Fitting. One of our purposes in this study is to propose a multivariable function that can fit the self-diffusion coefficient over the whole range of thermodynamic states in which the self-diffusion data exist. The function we propose is the one with the two variables, the density ρ and the temperature inverse T^{-1} (eq 2). The fitting curve and the experimental data for water are compared in Figure 2a. Equation 2 can reproduces the overall behavior of the temperature and the density dependencies of the experimental data; the rms deviation of the experimental data in each literature from the fitting curve is 4 % for the supercritical conditions in refs 17 and 18, 6 % for the supercritical conditions in ref 14, 7 % for the high-density data in ref 13, and 17 % for the high-density data in ref 11. The rms deviation of eq 2 along the liquid branch of the coexistence curve from $D_{ave,fit}$ obtained in eq 1 is 3 %. The dominant contribution to the large deviation for ref 11 is mostly coming from the high-density data at the low temperatures. Whereas eq 2 covers a wider range, eq 1 is more recommended for interpolation when only the data on the coexistence curve are of interest.

As shown by the enlarged view in Figure 2b, eq 2 provides smooth and reasonable temperature and density dependencies in the medium-density supercritical conditions. The data along the coexistence curve and those in the extremely low density region are essential for the reasonable fitting curves at the medium densities, because the data by Lamb et al.[14] have larger uncertainties in comparison to those in other conditions probably due to difficulties in the pressure control under extreme conditions. The realistic isothermal fitting curves in Figure 2b are obtained only when the data at lower and higher densities are available; when only the data in the supercritical states are fitted to eq 2, the resultant curve cannot smoothly reproduce the data points in the medium-density region (fitting result not shown).

The fitting in the form of eq 2 for benzene is shown in Figure 2c. The rms deviation of the experimental data in each literature from the fitting curve is 5 % for the supercritical conditions in ref 25, 4 % for the supercritical conditions in ref 24, 4 % for the high-density data in refs 20 and 21, and 6 % for the high-density data in ref 23. The rms deviation of eq 2 along the liquid branch of the coexistence curve from $D_{ave,fit}$ obtained by eq 2 is 1 %.

The fitting in the form of eq 2 for cyclohexane is shown in Figure 2d. The quality of the fitting shown in Figure 2d is not as good as those for water and benzene. The rms deviation of 6 % for fitting along the liquid branch of the coexistence curve is rather large, and the isothermal fitting curves at (300 and 400) °C intersect one another, leading to unreasonable temperature dependence of the scaled value $\rho D/T^{1/2}$ above the density

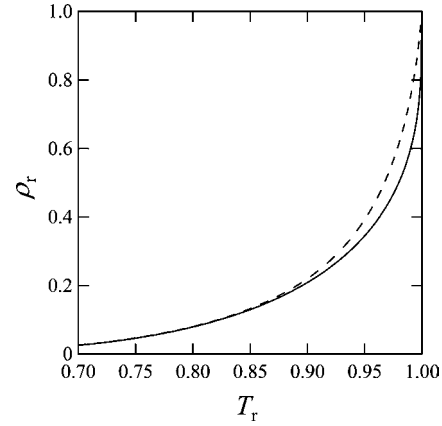

Figure 3. Reduced densities of benzene and cyclohexane along the gas branch of the coexistence curve as a function of the reduced temperature. The solid and dashed curves indicate the benzene and cyclohexane values, respectively.

of the intersection. These trends can be caused by a positive slope of $\rho D/T^{1/2}$ for cyclohexane against ρ. In general, the experimentally determined initial slopes for other substances are almost zero or slightly negative.[21,28,29,32−37] A slightly positive slope has been reported for xenon; however, the increase in $\rho D/T^{1/2}$ from the zero-density limit to the maximum was only 6 %, which is much smaller than the 20 % increase for cyclohexane at 400 °C shown in Figure 2d. Since the data for benzene and cyclohexane are taken from the same literature source,[25] the precision of the diffusion measurement for cyclohexane is the same as that for benzene, for which the initial slope of $\rho D/T^{1/2}$ is almost zero. A source of the unusual cyclohexane behavior can be its saturation vapor density data along the coexistence curve. The supercritical densities of the $\rho D/T^{1/2}$ in the low-density region were determined by those on the gas branch of the coexistence curve using the chemical-shift method.[25] Thus, when the vapor density for cyclohexane in literature[50] is overestimated, the $\rho D/T^{1/2}$ values can be overestimated accordingly. To test this possibility, in Figure 3 the reduced density ($\rho_r = \rho/\rho_c$) of the cyclohexane is compared to that for benzene as a function of the reduced temperature ($T_r = T/T_c$). Here the *PVT* data and the critical density ρ_c and temperature T_c are taken from refs 51 and 50 for benzene and cyclohexane, respectively. As is seen in Figure 3, ρ_r for cyclohexane becomes larger than that for benzene as it approaches the critical point, suggesting the overestimation of the cyclohexane vapor density at high temperatures.

It is of interest to examine whether the peculiar trend of $\rho D/T^{1/2}$ in Figure 2d is modified when the cyclohexane vapor density is replaced by the one obtained using the reduced density of benzene. In Figure 2e, we show $\rho D/T^{1/2}$ for cyclohexane with the low-density supercritical data recalculated based on the reduced density of benzene. The initial slope becomes almost zero, and the rms deviation along the coexistence curve is reduced from 6 % to 2 %. The isothermal curves at (300 and 400) °C have no intersection and have more reasonable, parallel behavior. The fitting quality for the other thermodynamic states is also improved when the density is replaced; the rms deviation is reduced from 6 % to 5 % for ref 25, from from 21 % to 23 % for ref 23, from 9 % to 4 % for ref 26, and from 14 % to 13 % for ref 27. The vapor density for cyclohexane obtained by using the reduced density of benzene is shown in SI (Table S1). A further improvement of the density data for cyclohexane along the gas branch of the coexistence curve is necessitated.

It is to be noted that the scaling procedure in terms of $\rho D/T^{1/2}$ plays a key role in obtaining a better fitting, in particular,

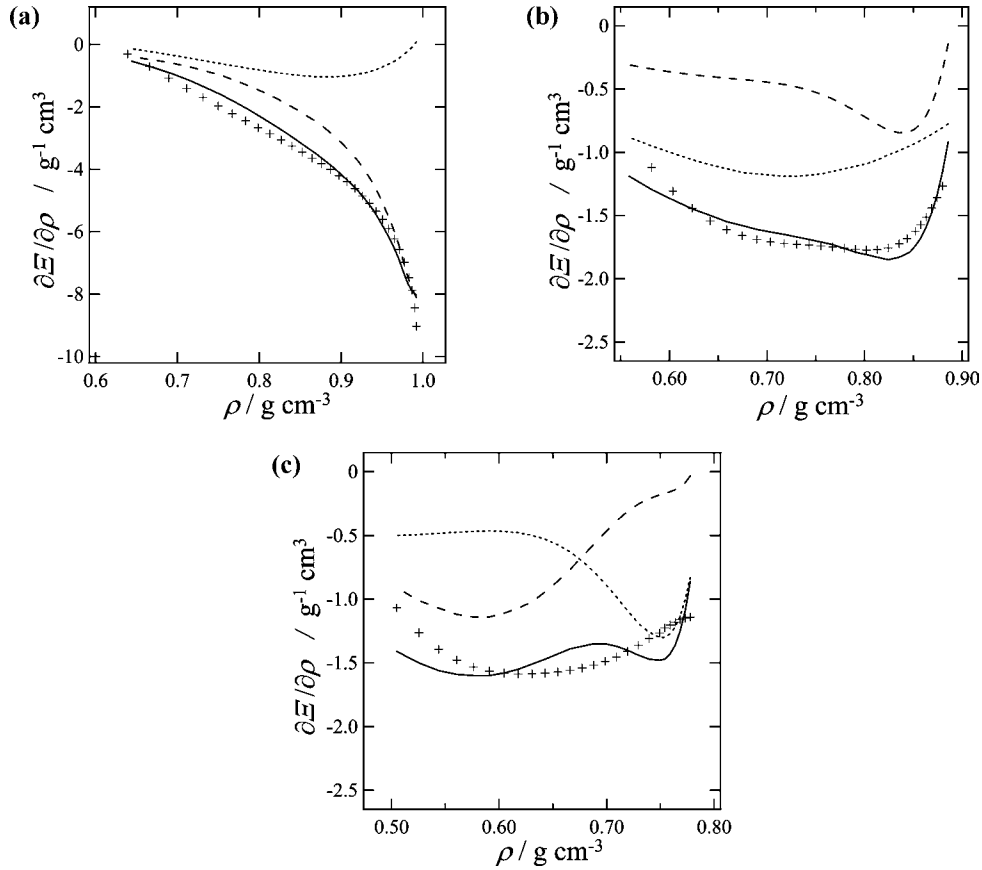

Figure 4. Density differential of the coefficient Ξ, $(\delta\Xi/\delta\rho)_{coex}$, obtained by differentiating eq 2 for (a) water, (b) benzene, and (c) cyclohexane. The dashed line, the dotted line, and the solid line indicate the fitting results of the T term, ρ term, and the sum of T and ρ terms, respectively. The crossed symbols (+) indicate the $(\delta\Xi/\delta\rho)_{coex}$ values obtained by the linear fitting of the three Ξ values at the neighboring temperatures.

including the extremely low density region. Although eq 2 appears to resemble the one proposed by Woolf and Collings,[21] not ln D but $\rho D/T^{1/2}$ is used, and higher-order terms are included in eq 2. Equation 2 fits the water data much better than the function proposed by them. This shows that the scaling in the form of $\rho D/T^{1/2}$ is of key importance in fitting the D values undergoing extensive changes.

3.2.2. Separation of Temperature and Density Effects. One of the important benefits of the functional form of eq 2 is that the temperature and the density derivatives can be examined even near the critical temperature. Here we examine the contributions of the temperature and the density effects on the self-diffusion coefficients along the liquid branch of the coexistence curve. Recently[19] a scheme was proposed to decompose the density and temperature effects into the analytical forms. In general, a physical quantity Ξ obtained along the coexistence curve can be decomposed into the two terms associated with the isochoric and isothermal differentials as follows:

$$\left(\frac{\partial\Xi}{\partial\rho}\right)_{coex} = \left(\frac{\partial\Xi}{\partial T}\right)_{\rho}\left(\frac{\partial T}{\partial\rho}\right)_{coex} + \left(\frac{\partial\Xi}{\partial\rho}\right)_{T} \quad (4)$$

The first and the second terms of the right-hand side of eq 4 are called as the T term and the ρ term, respectively. A dimensionless coefficient Ξ for the self-diffusion is defined as

$$\rho D/\sqrt{T} = \Xi(\rho D/\sqrt{T})^* \quad (5)$$

where $(\rho D/T^{1/2})^*$ is set to 1 mg·m^{-1}·s^{-1}·K$^{-1/2}$. In the previous work[19] we investigated the contributions of the T and the ρ terms by carrying out curve-fitting of the experimentally obtained numerical values of $(\delta\Xi/\delta\rho)_{coex}$, on the assumption that the temperature and density dependencies of $(\delta\Xi/\delta T)_{\rho}$ and $(\delta\Xi/\delta\rho)_{T}$ are not essential for the discussion, the two partial differentials, $(\delta\Xi/\delta T)_{\rho}$ and $(\delta\Xi/\delta\rho)_{T}$, were treated as constant parameters. The $P-\rho-T$ related quantities along the coexistence curve, $(\delta T/\delta\rho)_{coex}$, were taken from the literature.[50−52] Now that we have formulated the explicit function of temperature and density, we can examine $(\delta\Xi/\delta T)_{\rho}$ and $(\delta\Xi/\delta\rho)_{T}$ by utilizing the explicit function of density and temperature (eq 2). Since $(\delta\Xi/\delta T)_{\rho}$ and $(\delta\Xi/\delta\rho)_{T}$ are obtained from the differentials of eq 2, the temperature and density dependencies of $(\delta\Xi/\delta T)_{\rho}$ and $(\delta\Xi/\delta\rho)_{T}$ can be discussed quantitatively.

In Figure 4a, we show the T and the ρ terms for water in eq 2. The absolute value of $(\delta\Xi/\delta\rho)_{coex}$ is large in the vicinity of the ambient conditions, representing the large change of the self-diffusion coefficient for water along the coexistence curve near room temperature. The plot of $(\delta\Xi/\delta\rho)_{coex}$ values steeply rises with decreasing density as a result of the breakage of the hydrogen bonding that lowers the barrier height for the diffusion of water molecules. The T and ρ term separation indicates that both of the absolute values are large in the ambient conditions, making the absolute value of $(\delta\Xi/\delta\rho)_{coex}$ large. The T term shows a more dramatic change with density reduction than the ρ term, because the change in the T term is caused by $(\delta T/\delta\rho)_{coex}$. Therefore, the steep rise in $(\delta\Xi/\delta\rho)_{coex}$ with decreasing density comes from the T terms. This is a remarkable feature of water diffusion clarified below by the comparison with the organic liquids. In contrast, the contribution of the ρ term is small at lower temperatures. The value of the ρ term for water is slightly positive below room temperature due to the enhancement of the self-diffusion due to the distortion and breakage of the hydrogen bonding upon the compression.

In Figure 4b,c, the coefficients $(\delta\Xi/\delta\rho)_{coex}$ for benzene and cyclohexane are plotted against density, respectively. In the case of the cyclohexane, the T and ρ terms were obtained from the fitting curve with the density correction for the supercritical data (Figure 2e). Benzene differs from water in the temperature effect. The smaller variations of $(\delta\Xi/\delta\rho)_{coex}$ for organic liquids are due to the fact that the weight of the T term at low temperatures is smaller than that for water. A marked contrast between water and benzene corresponds well to the interpretation of the computational analysis based on the dynamic solvation shell model.[39] As found only in water, the temperature effect on the D arises from the dramatic turnover from the in-shell (velocity relaxation within the solvation shell) to the mobile-shell (the solvation shell relaxation faster than the velocity relaxation) type. In benzene, the large, repulsive obstruction effect in highly packed conditions plays the main role in controlling the solvation dynamics to confine the relaxation of translational velocity within the shell. Temperature variation has little effect on such repulsive effects, and thus the benzene diffusion at the ambient density is of the in-shell type up to such a high temperature as 400 °C.[39]

4. Conclusions

The self-diffusion coefficients D in sub- and supercritical fluids determined are collected, evaluated, and formulated in high-temperature conditions over a wide range of density. The Arrhenius type with the fifth-order polynomial of T^{-1} (eq 1) is proposed for the fitting function for the evaluated experimental data on the liquid branch of the coexistence curve. As indicated by eq 2 both variables, density and temperature, are necessary for the good fit over the wide range of temperature and density including the extremely low density supercritical region. Equation 2 in the scaled form is found to be also useful for estimating the self-diffusion coefficients in the supercritical states at medium- to high densities. The separation of density and temperature effects on D was accomplished by differentiating the analytical function obtained. The temperature effect on water is much larger than that on benzene and cyclohexane because of the presence of the hydrogen bonding. The scaled expression obtained here can be used for the extrapolation guided by molecular dynamics simulation to the experimentally inaccessible conditions, under which the kinetic energy of fluids at extremely high temperatures is to be transformed into the mechanical through the electromagnetic effect in the high-efficiency power generation.

Acknowledgment

This paper is dedicated to Joseph M. G. Barthel.

Supporting Information Available:

Table of cyclohexane density obtained based on ref 51. Figure S1 shows the deviations of the self-diffusion coefficients in literature, and Figure S2 shows the Arrhenius plot of the self-diffusion coefficient. This material is available free of charge via the Internet at http://pubs.acs.org.

Literature Cited

(1) Hirschfelder, J. O.; Curtiss, C. F.; Bird, R. B. *Molecular Theory of Gases and Liquids*; Wiley: New York, 1954.
(2) Chapman, S.; Cowling, T. G. *The mathematical theory of non-uniform gases*, 3rd ed.; Cambridge University Press: London, 1970.
(3) Tyrrell, H. J. V.; Harris, K. R. *Diffusion in Liquids*; Butterworths: London, 1984.
(4) Hansen, J. P.; McDonald, I. R. *Theory of Simple Liquids*; Academic Publishers: London, 1986.
(5) Matubayasi, N.; Wakai, C.; Nakahara, M. Structural study of supercritical water I. Nuclear magnetic resonance spectroscopy. *J. Chem. Phys.* **1997**, *107*, 9133–9140.
(6) Matubayasi, N.; Wakai, C.; Nakahara, M. Structural study of supercritical water. II. Computer simulations. *J. Chem. Phys.* **1999**, *110*, 8000–8011.
(7) Tassaing, T.; Cabaço, M. I.; Danten, Y.; Besnard, M. The structure of liquid and supercritical benzene as studied by neutron diffraction and molecular dynamics. *J. Chem. Phys.* **2000**, *113*, 3757–3765.
(8) Hausser, R.; Maier, G.; Noack, F. Kernmagnetische messungen von selbstdiffusions-koeffizienten in wasser und benzol bis zum kritischen punkt. *Z. Naturforsch., A* **1966**, *21*, 1410–1415.
(9) Gillen, K. T.; Douglass, D. C.; Hoch, M. J. R. Self-Diffusion in Liquid Water to −31 °C. *J. Chem. Phys.* **1972**, *57*, 5117–5119.
(10) Mills, R. Self-diffusion in normal and heavy water in the range 1−45°. *J. Phys. Chem.* **1973**, *77*, 685–688.
(11) Wilbur, D. J.; DeFries, T.; Jonas, J. Self-diffusion in compressed liquid heavy water. *J. Chem. Phys.* **1976**, *65*, 1783–1786.
(12) Krynicki, K.; Green, C. D.; Sawyer, D. W. Pressure and temperature dependence of self-diffusion in water. *Discuss. Faraday Soc.* **1978**, *66*, 199–208.
(13) Harris, K. R.; Woolf, L. A. Pressure and temperature dependence of the self diffusion coefficient of water and oxygen-18 water. *J. Chem. Soc., Faraday Trans. 1* **1980**, *76*, 377–385.
(14) Lamb, W. J.; Hoffman, G. A.; Jonas, J. Self-diffusion in compressed supercritical water. *J. Chem. Phys.* **1981**, *74*, 6875–6880.
(15) Easteal, A. J.; Price, W. E.; Woolf, L. A. Diaphragm cell for high-temperature diffusion measurements. Tracer Diffusion coefficients for water to 363 K. *J. Chem. Soc., Faraday Trans. 1* **1989**, *85*, 1091–1097.
(16) Holz, M.; Heil, S. R.; Sacco, A. Temperature-dependent self-diffusion coefficients of water and six selected molecular liquids for calibration in accurate ^{1}H NMR PFG measurements. *Phys. Chem. Chem. Phys.* **2000**, *2*, 4740–4742.
(17) Yoshida, K.; Wakai, C.; Matubayasi, N.; Nakahara, M. A new high-temperature multinuclear-magnetic-resonance probe and the self-diffusion of light and heavy water in sub- and supercritical conditions. *J. Chem. Phys.* **2005**, *123*, 164506 (10 pages).
(18) Yoshida, K.; Matubayasi, N.; Nakahara, M. Self-diffusion of supercritical water in extremely low-density region. *J. Chem. Phys.* **2006**, *125*, 074307 (7 pages); **2007**, 126 089901 (2 pages).
(19) Yoshida, K.; Matubayasi, N.; Nakahara, M. Self-diffusion coefficients for water and organic solvents at high temperatures along the coexistence curve. *J. Chem. Phys.* **2008**, *129*, 214501.
(20) McCool, M. A.; Collings, A. F.; Woolf, L. A. Pressure and temperature dependence of the self-diffusion of benzene. *J. Chem. Soc., Faraday Trans. 1* **1972**, *68*, 1489–1497.
(21) Collings, A. F.; Woolf, L. A. Self-diffusion in benzene under pressure. *J. Chem. Soc., Faraday Trans. 1* **1975**, *71*, 2296–2298.
(22) Parkhurst, H. J.; Jonas, J. Dense liquids. I. The effect of density and temperature on self-diffusion of tetramethylsilane and benzene-d_6. *J. Chem. Phys.* **1975**, *63*, 2698–2704.
(23) Polsin, B.; Weiss, A. Transport properties of liquids. VIII. Molar volume and self diffusion of organic liquids at pressures up to 200 MPa. *Ber. Bunsen-Ges.* **1990**, *94*, 746–758.
(24) Asahi, N.; Nakamura, Y. NMR study of liquid and supercritical benzene. *Ber. Bunsen-Ges.* **1997**, *101*, 831–836.
(25) Yoshida, K.; Matubayasi, N.; Nakahara, M. Self-diffusion coefficients for water and organic solvents in extremely low-density supercritical states. *J. Mol. Liq.* **2009**, *147*, 96–101.
(26) McCool, M. A.; Woolf, L. A. Self-diffusion measurements under pressure with a diaphragm cell. Theory of the method, and experimental results for cyclohexane. *High Temp. High Pressures* **1972**, *4*, 85–95.
(27) Jonas, J.; Hasha, D.; Huang, S. G. Density effects of transport properties in liquid cyclohexane. *J. Phys. Chem.* **1980**, *84*, 109–112.
(28) O'Hern, H. A.; Martin, J. J. Diffusion in Carbon Dioxide at Elevated Pressures. *Ind. Eng. Chem.* **1955**, *47*, 2081–2087.
(29) Takahashi, S.; Iwasaki, H. The Diffusion of Gases at High Pressures. I. The Self-diffusion Coefficient of Carbon Dioxide. *Bull. Chem. Soc. Jpn.* **1966**, *39*, 2105–2109.
(30) Dawson, R.; Khoury, F.; Kobayashi, R. Self-diffusion in methane by pulsed nuclear magnetic resonance. *AIChE J.* **1970**, *16*, 725–729.
(31) Khoury, F.; Kobayashi, R. Data by NMR and representations of self-diffusion coefficients in carbon tetrafluoride and the determination of intermolecular force constants. *J. Chem. Phys.* **1971**, *55*, 2439–2445.
(32) Oosting, P. H.; Trappeniers, N. J. Proton-spin-lattice relaxation and self-diffusion in methanes IV. Self-diffusion in methane. *Physica (Amsterdam, Neth.)* **1971**, *51*, 418–431.
(33) Trappeniers, N. J.; Michels, J. P. J. The density dependence of the self-diffusion coefficient of krypton. *Chem. Phys. Lett.* **1973**, *18*, 1–3.

(34) Harris, K. R. The density dependence of the self-diffusion coefficient of methane at−50°, 25° and 50 °C. *Physica A (Amsterdam, Neth.)* **1978**, *94*, 448–464.
(35) Harris, K. R. The density dependence of the self-diffusion coefficient of chlorotrifluoromethane near the critical temperature. *Physica A (Amsterdam, Neth.)* **1978**, *93*, 593–610.
(36) Arends, B.; Prins, K. O.; Trappeniers, N. J. Self-diffusion in gaseous and liquid ethylene. *Physica A (Amsterdam, Neth.)* **1981**, *107*, 307–318.
(37) Peereboom, P. W. E.; Luigjes, H.; Prins, K. O. An NMR spin-echo study of self-diffusion in xenon. *Physica A (Amsterdam, Neth.)* **1989**, *156*, 260–276.
(38) Etesse, P.; Zega, J. A.; Kobayashi, R. High pressure nuclear magnetic resonance measurement of spin-lattice relaxation and self-diffusion in carbon dioxide. *J. Chem. Phys.* **1992**, *97*, 2022–2029.
(39) Yoshida, K.; Matubayasi, N.; Nakahara, M. Solvation shell dynamics studied by molecular dynamics simulation in relation to the translational and rotational dynamics of supercritical water and benzene. *J. Chem. Phys.* **2007**, *127*, 174509 (13 pages).
(40) Nagai, Y.; Morooka, S.; Matubayasi, N.; Nakahara, M. Mechanisms and kinetics of acetaldehyde reaction in supercritical water: Noncatalytic disproportionation, condensation, and decarbonylation. *J. Phys. Chem. A* **2004**, *108*, 11635–11643.
(41) Morooka, S.; Wakai, C.; Matubayasi, N.; Nakahara, M. Hydrothermal carbon-carbon bond formation and disproportionations of C1 aldehydes: formaldehyde and formic acid. *J. Phys. Chem. A* **2005**, *109*, 6610–6619.
(42) Matubayasi, N.; Nakahara, M. Hydrothermal reactions of formaldehyde and formic acid: Free-energy analysis of equilibrium. *J. Chem. Phys.* **2005**, *122*, 074509 (12 pages).
(43) Yasaka, Y.; Yoshida, K.; Wakai, C.; Matubayasi, N.; Nakahara, M. Kinetic and equilibrium study on formic acid decomposition in relation to the water-gas-shift reaction. *J. Phys. Chem. A* **2006**, *110*, 11082–11090.
(44) Morooka, S.; Matubayasi, N.; Nakahara, M. Kinetic study on disproportionations of C1 aldehydes in supercritical water: methanol from formaldehyde and formic acid. *J. Phys. Chem. A* **2007**, *111*, 2697–2705.
(45) McQuarrie, D. A. *Statistical Mechanics*, 2nd revised ed.; University Science Books: Sausalito, CA, 2000.
(46) Holz, M.; Mao, X.-A.; Seiferling, D. Experimental study of dynamic isotope effects in molecular liquids: Detection of translation-rotation coupling. *J. Chem. Phys.* **1996**, *104*, 669–679.
(47) Hardy, E. H.; Zygar, A.; Zeidler, M. D.; Holz, M.; Sacher, F. D. Isotope effect on the translational and rotational motion in liquid water and ammonia. *J. Chem. Phys.* **2001**, *114*, 3174–3181.
(48) Buchhauser, J.; Gross, T.; Karger, N.; Lüdemann, H.-D. Self-diffusion in CD_4 and ND_3: With notes on the dynamic isotope effect in liquids. *J. Chem. Phys.* **1999**, *110*, 3037–3042.
(49) Chen, L.; Gross, T.; Krienke, H.; Lüdemann, H.-D. *T,p*-Dependence of the self-diffusion and spin-lattice relaxation in fluid hydrogen and deuterium. *Phys. Chem. Chem. Phys.* **2001**, *3*, 2025–2030.
(50) Penoncello, S. G.; Jacobsen, R. T.; Goodwin, A. R. H. A thermodynamic property formulation for cyclohexane. *Int. J. Thermophys.* **1995**, *16*, 519–531.
(51) Goodwin, R. D. Benzene thermophysical properties from 279 to 900 K at pressures to 1000 bar. *J. Phys. Chem. Ref. Data* **1987**, *17*, 1541–1636.
(52) Wagner, W.; Pruss, A. The IAPWS Formulation 1995 for the Thermodynamic Properties of Ordinary Water Substance for General and Scientific Use. *J. Phys. Chem. Ref. Data* **2002**, *31*, 387–535.

Received for review November 26, 2009. Accepted April 28, 2010. This work is supported by the Grants-in-Aid for Scientific Research (Nos. 18350004, 21300111, and 21850021) from the Japan Society for the Promotion of Science and by the Grant-in-Aid for Scientific Research on Innovative Areas (20118002) and the Next-Generation Integrated Nanoscience Simulation Software Project from the Ministry of Education, Culture, Sports, Science, and Technology. N.M. is also grateful for the grant from the Association for the Progress of New Chemistry, the grant from the Suntory Institute for Bioorganic Research, and the Supercomputer Laboratory of Institute for Chemical Research, Kyoto University. M.N. further acknowledges the donation of The Water Chemistry Energy Laboratory (AGC) from Asahi Glass Co., Ltd.

JE100206S